Computer-AidedDesign

Taylor & Francis
Taylor & Francis Group

An energy saving approach for rough milling tool path planning

Ke Xu ⬤ and Kai Tang ⬤

Hong Kong University of Science and Technology, Hong Kong

ABSTRACT

For a specific machine configuration, energy consumption in a rough milling process is strongly affected by three parameters: axial depth of cut, radial depth of cut and feed rate. On the other hand, feed rate is also physically constrained by a critical cutting force value. Based on these concerns, we establish an energy consumption formula as a function of the three, aiming to find out the optimal set of parameters which is the most energy-efficient. After that, two strategies, i.e. improved constant Z-level strategy and optimized morphing strategy for tool path generation in terms of 3-axis ball-end milling are thus presented based on the previous obtained parameters. Simulation show that the optimal parameters together with the proposed tool path generation methods can save up to 30% of the total energy usage compared with traditional cutting parameters in rough milling.

1. Introduction

Sustainable development has been highlighted as one of the main target since the beginning of the 21th century. When it comes into CNC machining, usually a large amount of energy will be consumed or unnecessarily wasted when machining molds or blades with large scale, especially for the first stage, i.e. the rough milling process. In the early days, researchers have dedicated to improving machining efficiency so as to enlarge the productivity, intuitively this might also lower the energy consumption if we assume the total machine power to be a fixed value. However, to think further, in order to increase the machining efficiency, a resultant large material removal rate (MRR) will be inevitably produced, which in turn generate a higher cutting force and increase the actual cutting power demand. As an initial guess, to some extent, high machining efficiency and energy performance might conflict with each other. Therefore, the goal of this paper is to reveal the inner connection between these two objectives and give a convincing solution to the energy concern.

1.1. Outcomes in energy consumption modeling

The energy consumption in CNC machining is too complicated to predict theoretically, previous researchers have revealed the inner-relationship between specific energy and material removal rate (MRR) experimentally. Kara and Li [11] proposed an empirical approach to calibrate the energy consumption model in terms of process variables, according to their models of 4 types of machine tools, a larger MRR results in a significant energy saving, and dry cut is much more energy efficient than wet cut. A similar model has been proposed in [3], a group of cutting tests with different depth of cut show the decreasing in processing time dominates over the increasing power caused by a larger load. Draganescu et al. [6] built up a statistic model of machine efficiency and specific energy as a unary function of different working parameters, from which the specific energy can be determined by a given set of parameters. However this model is only valid for a specific machine configuration and it is impossible to reach the global optimal working parameters by unary function. Therefore, other studies focusing on energy optimization came out with a variety of approaches. Based on hundreds of experiments, Quintana et al. [24] developed an artificial neural network (ANN) to predict power consumption and the most effective cutting parameters, results show that a lower spindle speed with a larger feed per tooth value are preferred for a low power consumption. The relation between specific power and cutting width and cutting height has been plotted in [4], however there shows no mathematical description for this relationship. Other research such as [20] and [21] presented different production planning ways to make an efficient process control. To sum up, although there exist different ways to determine a plausible set of energy-saving parameters, none of them have

---

CONTACT Ke Xu ✉ kxuae@ust.hk

considered the physical limits of machine, if the optimal parameters happen to exceed the machine tool capacity in real machining, tool damage might occur.

1.2. Studies in terms of machine capacity

To get the feasible cutting parameters in terms of energy saving, the physical capacities of machine should be considered. Two mostly concerned aspects are the cutting mechanics and the machine kinematic limits. In respect of kinematics, feed rate between adjacent CL points should be smoothly assigned due to the acceleration and jerk constraints of the machine. Most studies such as [2, 13, 25] focused on five-axis feed rate optimization. However in 3-axis roughing process, tool paths are simply low degree curves or straight lines where the kinematic capacity is unlikely to be exceeded, yet large chip load turns the attention to the other side, i.e. the cutting force constraint.

Past researchers have presented a number of cutting force models for both end milling and flank milling [1, 7, 12, 15, 17, 22, 23], including both analytical and numerical ways to calculate cutting force. Based on these models, some feed rate scheduling techniques have been proposed in CNC stage. [14] reviewed both MRR-based and force-based feed rate scheduling strategies, the latter is more convincing and accurate. Erdim et al.[8] regulated feed rate under a reference cutting force constraint and verified their results in a vertical machine center. Feng and Su [9] proposed an integrated way to enlarge productivity for 3-axis machining, by firstly generating the constant scallop height tool paths and then maximize the feed rate along the tool path by cutting force constraint. A five-axis feed rate scheduling method was raised by [28], example of an impeller blade machining show a reduction of 35% in total machining time can be reached after rescheduling the feed rate.

1.3. Tool path strategies

Assume we have obtained the optimal cutting parameters, the afterward tool path generation should be finalized in CAM stage. Numerous strategies have been proposed to generate tool path for free-form surface finishing, such as iso-planar [5], constant scallop height [19, 26], and iso-phote strategy [10]. One similarity of these approaches is that only one layer of tool paths is generated. Considering a multi-layer machining process in rough milling, a traditional way is to apply a 2D pocket strategy for each layer. [27] compared three path fashions (offset, raster, single direction raster) of pocket machining in order to achieve a high productivity, the raster strategy is mostly preferred for a larger MRR and

longer tool life. Besides, morphing technique has been transformed into tool path planning to eliminate the 'stairs' left on surface. [18] gave two reasonable morphing strategies: linear interpolation and Hermit interpolation to produce roughing levels in 3-axis machining. Lauwers and Lefebvre [16] extended this idea into 5-axis machining, gauge free tool paths can be generated in a smoother fashion.

To sum up, a number of energy models, feed rate scheduling techniques and tool path generation methods have been proposed by past studies. However, to really make a feasible planning for energy saving, we have to link all these aspects up to make an integrated optimization. The following parts of this paper will turn this thought into reality step by step. To start with, section 2 will introduce an enhanced energy consumption model which takes mechanics constraints into consideration, based on which the optimal cutting parameters can be obtained. In phase 2, according to the optimal parameters, section 3 will describe two different strategies for 3-axis tool path planning. After that, a benchmark test will be carried out between traditional and optimal cutting parameters in both tool path strategies.

2. Energy consumption model

Energy consumption is a very complicated mechanism during the machining process, the power demand for every single component varies with different machine configuration and tool shape. Each machine will have a unique energy consumption model (ECM), which makes it impossible to cover all the existing machine types and derive their own ECM repeatedly, therefore in this section, a general form of ECM for 3-axis ball-end milling process will be proposed so that one can easily adapt to a specific machine tool after a careful calibration.

Regardless of the machine type, the power demand for any machining process can be divided into two parts: the idle power demand and the cutting power demand. A number of components such as servo, lighting, spindle, etc. consume energy as long as the machine is powered on, these energy usage can be classified into the idle power demand, which is normally assumed fixed during a single machining process. However in terms of the cutting power demand, the value changes greatly due to different cutting parameters. In the following part of this section, a thorough derivation in terms of the cutting power demand will be given in 2.1, and a combination of the two power demands will be proposed in 2.2, where a global formula for energy consumption will thus be derived.

2.1. Specific cutting energy

Theoretically, the specific cutting energy (SCE) is the value of energy consumption when the tool cuts a unit volume of material. Regardless of the machine configuration, SCE only varies with tool shape, axial and radial depth of cut (a_p & a_e), and feed per spindle turn (f_t), which can be formulated as the following equation:

$$SCE = \frac{E_s(f_t, a_e, a_p)}{V_s(f_t, a_e, a_p)} \tag{2.1}$$

Where: E_s and V_s are the consumed cutting energy and the swept material volume during one spindle turn, respectively. As a consequence, for a given tool, SCE is a function of the three variables.

In order to derive the expression of SCE in terms of a_p, a_e and f_t, a cutting model for three axis ball-end milling should be built up first. Generally, the tool moves in a zig-zag or a contour fashion and cuts the material layer by layer, ignore the first layer, in most of the time the tool encounters the unfinished workpiece with its left (or right) side and its top surface already been machined by the previous cuts. The figure below shows a transient state of the cutting process in a 2D fashion, where the shaded area represents the cutter-workpiece engagement (CWE) region, which is highly influenced by the previous cut.

Based on this assumption, we are now able to formulate E_s and V_s individually. Basically, E_s is equal to the total work done by cutting force per spindle turn, therefore the cutting force model is presented in the first place:

$$\begin{pmatrix} dF_t \\ dF_r \\ dF_a \end{pmatrix} = \begin{pmatrix} K_{tc} \cdot T(f_t, \varphi, \kappa) \cdot db + K_{te} \cdot dS \\ K_{rc} \cdot T(f_t, \varphi, \kappa) \cdot db + K_{re} \cdot dS \\ K_{ac} \cdot T(f_t, \varphi, \kappa) \cdot db + K_{ae} \cdot dS \end{pmatrix}$$

$$db = \frac{dz}{\sin \kappa},$$

$$dS = \sqrt{(R'(\varphi)^2 + R^2(\varphi) + R_0^2 \cot^2(i_0))}d\varphi \tag{2.2}$$

$$\begin{bmatrix} dF_u \\ dF_v \\ dF_w \end{bmatrix} = \begin{bmatrix} -\sin(\kappa)\sin(\varphi) & -\cos(\varphi) & -\cos(\kappa)\sin(\varphi) \\ -\sin(\kappa)\cos(\varphi) & \sin(\varphi) & -\cos(\kappa)\cos(\varphi) \\ \cos(\kappa) & 0 & -\sin(\kappa) \end{bmatrix}$$
$$\begin{bmatrix} dF_r \\ dF_t \\ dF_a \end{bmatrix} \tag{2.3}$$

Fig. 2 and Eqn. (2.2) show the differential cutting force model originally proposed by Lee and Altintas [17], where $R(\varphi)$ is the radius of the cutting plate starting from 0 to R_0. The differential tangent (dF_t), radial (dF_r) and subtangent (dF_a) cutting force are the three orthogonal vectors acting on a single point along the cutting edge.

Eqn. (2.3) expresses the orthogonal decomposed cutting force in the tool coordinate system, κ and φ are respectively the immersion and rotational angle to define the position of the cutting edge, i_0 is the helix angle. The edge coefficients (K_{te} K_{re} K_{ae}) and the shearing coefficients (K_{tc} K_{rc} K_{ac}) vary with different materials and cutters. Details of this model can be found in [17], while the value of the six coefficients in terms of a specified material is carefully calibrated.
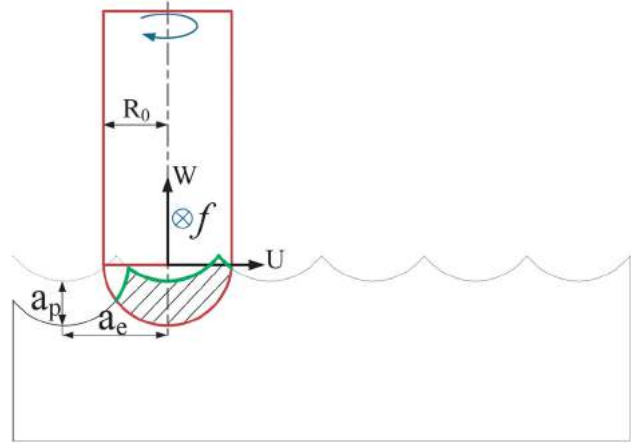

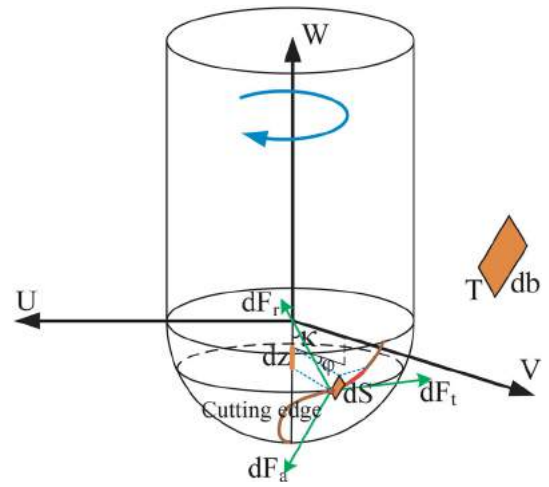**Figure 1.** Cutting parameters and engagement region of three axis ball-end milling.

Figure 2. Differential cutting force exerted on one point.

The next step is to derive the cutting motion as a function of the rotational angle φ. The actual motion of one cutting edge, especially in conventional CNC machining, is not just a simple rotation but a combined movement of spindle rotation and translation, one possible trajectory for a specified point on cutting edge is shown below:

From Fig. 3, it is clear that the cutting edge moves in a screw-like trajectory, therefore the concerned point on
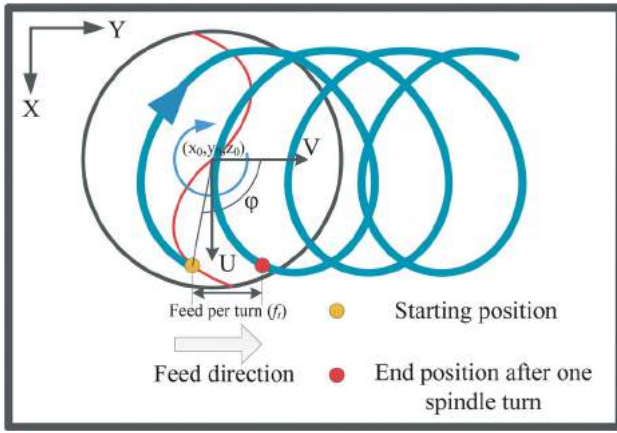
Figure 3. Trajectory of one point on the cutting edge.

the cutting edge will translate a distance of feed per spindle turn f_t after one spin, the expression of this trajectory in terms of φ in the workpiece coordinate system is:

$$\vec{S}(\kappa,\varphi) = \begin{pmatrix} x_p \\ y_p \\ z_p \end{pmatrix} = \begin{pmatrix} x_0 + R_0\sin(\kappa)\sin(\varphi) \\ y_0 + R_0\sin(\kappa)\cos\varphi + f_t\frac{\varphi-\varphi_0}{2\pi} \\ z_0 - R_0\cos\kappa \end{pmatrix}$$

$$(2.4)$$

Obviously, energy consumption should be the product of force and displacement, the differential form is expressed by the following equation:

$$\int dE = \int \vec{F}\cdot \vec{dS} \tag{2.5}$$

Therefore, a similar form for the E_s can be derived with Eqn. (2.3), (2.4) and (2.5):

$$E_s(f_t,a_e,a_p) = \int_{-R_0}^{l-R_0}\int_{\varphi_0}^{\varphi_0+2\pi} \begin{pmatrix} dF_u \\ dF_v \\ dF_w \end{pmatrix}\cdot\begin{pmatrix} dx_p \\ dy_p \\ dz_p \end{pmatrix}$$

$$= \int_{-R_0}^{l-R_0}\int_{\varphi_0}^{\varphi_0+2\pi} (R\sin(\kappa)\cos(\varphi)dF_u$$

$$+ \left(-R\sin(\kappa)\sin(\varphi) + \frac{f_t}{2\pi}\right)dF_v\right)d\varphi$$

$$(2.6)$$

This expression is a double integral in terms of $d\varphi$ and dz, where dz is hidden in dF_u and dF_v, meaning that after we get the differential energy usage for one single cutting point, the whole energy consumption can be calculated by a subsequent integral along the cutting edge. According to Fig. 1, dF_u and dF_v will be null if the concerned cutting point (u_p, v_p, w_p) locates outside the CWE (bounded by the green arcs).

Consequently, the cutting energy consumption E_s can be determined by Eqn. (2.6). Next, we will derive the

expression of V_s, i.e. the swept volume during one spindle turn.

Previously we have mentioned the engagement region as a projection form in 2D plane, Fig. 4 shows this region in both 3D and 2D fashion, where A and A_{pro} are their corresponding area. Obviously after one spindle turn, every point on the cutter will move a same distance of f_t along the feed direction, therefore for an infinitesimal area in the engagement region, its infinitesimal swept volume will be:

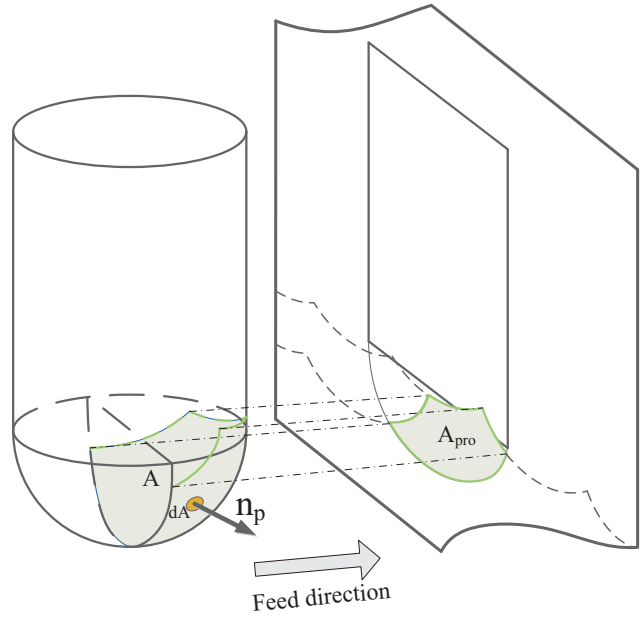$$dV = (\vec{n_p}\cdot\vec{f_t})dA \tag{2.7}$$

Figure 4. Cutter-workpiece engagement region in 3D fashion.

Where: $\vec{n_p}$ is the unit normal of dA. The whole swept volume should be the surface integral of the infinitesimal volume among the engagement region. Mathematically, the integral can be simplified as the product of the projection area A_{pro} and the travel distance f_t:

$$V_s(f_t,a_e,a_p) = \int_A dV = \int_A (\vec{n_p}\cdot\vec{f_t})dA = A_{pro}f_t \tag{2.8}$$

After that, the expression of the projection area A_{pro} in terms of a_e and a_p can be easily obtained by a reshaping trick shown in Fig. 5.

By the above methods, a complex swept volume can be simplified as follows:

$$V_s(f_t,a_e,a_p) = A_{pro}f_t = a_e a_p f_t \tag{2.9}$$

Also, an instantaneous material removal rate can be expressed as the product of V_s and spindle speed S:

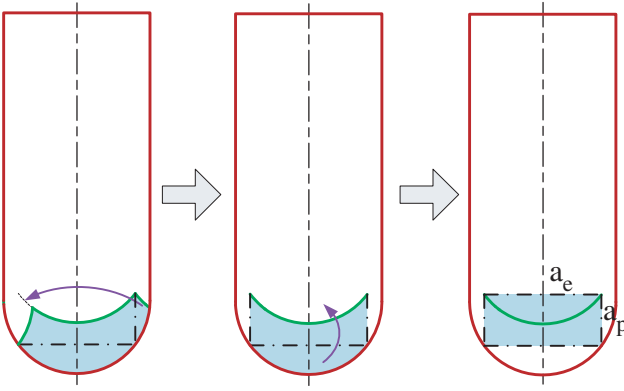$$MRR = \frac{V_s S}{60} = \frac{a_e a_p f_t S}{60} \tag{2.10}$$

Figure 5. Reshape the 2D engagement region.

So far, we have derived the cutting energy E_s and swept volume V_s in Eqn. (2.6), (2.7) and (2.10), substitute these two expressions back into Eqn. (2.1), we can finalize the SCE.

2.2. Global energy consumption formula (GEF)

In a macroscopic view, apart from the cutting energy, there also exists another type of energy consumption to cover the idle power demand as we introduced in the beginning of this section. Unlike the cutting energy model, it is impossible to get the mathematical model for the idle power demand due to the complexity of machine configuration, therefore a simplification is made in this paper that the idle power demand is assumed to be constant during the whole machining process, denoted by P_{idle}.

Based on this assumption, the longer machining time T, the more energy will be consumed by idle power demand. Given a raw block, the total volume of material to be removed V_r is fixed, so the total energy consumption E is:

$$E(f_t, a_e, a_p) = P_{idle}T + SCE \cdot V_r = \left(\frac{P_{idle}}{MRR} + SCE\right) V_r \tag{2.11}$$

Where: MRR is the mean material removal rate, thus the total machining time is the quotient of V_r over MRR, divide both sides of Eqn. (2.12) with V_r, we will get the specific energy consumption in the global view, defined as the global energy consumption formula (GEF):

$$GEF(f_t, a_e, a_p) = \frac{E}{V_r} = \frac{P_{idle}}{MRR} + SCE = \frac{60P_{idle}}{a_e a_p f_t S} + SCE(a_e, a_p, f_t) \tag{2.12}$$

In fact, P_{idle} is a constant, SCE and MRR are functions of f_t, a_e and a_p, therefore GEF is also a function of these

three variables, the final issue is to find out the optimal values for the three parameters for the minimization of GEF.

In rough milling, a larger MRR is always preferred, however this value is physically constrained by a critical value of cutting force. According to the previous cutting force model, with a given set of a_p&a_e, the peak value of cutting force during one cycle is actually a linear function of f_t:

$$F_{peak} = A(a_p, a_e)f_t + B(a_p, a_e) \tag{2.13}$$

Where: A, B are the coefficients of this linear function, varying with different set of a_p&a_e. Due to the physical constrain, if a threshold value F_0 is given, then the largest allowable $f_{t(max)}$ should be:

$$f_{t(max)}(a_e, a_p) = \frac{F_0 - B(a_p, a_e)}{A(a_p, a_e)} \tag{2.14}$$

Substitute Eqn. (2.14) back into Eqn. (2.12), a final expression of GEF as a function of two variables $(a_p$&$a_e)$ is presented below:

$$GEF(a_p, a_e) = \frac{60P_{idle}}{a_e a_p \frac{F_0 - B(a_p, a_e)}{A(a_p, a_e)} S} + SCE\left(a_e, a_p, \frac{F_0 - B(a_p, a_e)}{A(a_p, a_e)}\right) \tag{2.15}$$

As long as the machine configuration is specified and the workpiece material is given, we can always find out an optimal set of a_p&a_e to obtain the minimal value of GEF. For a particular case of a ball-end cutter with radius of 6 mm, 4 cutting edge and a helix angle of 30 degree, when the spindle speed is 3000 rpm and the workpiece is simple aluminum block, the relationship between GEF and a_p&a_e is shown in Fig. 6.

As we may observe from this figure, there should be an upper bound for a_p & a_e, since a large value of a_e will cause a bad surface quality (large cusp height), and the value of a_p should also be constrained by the length of the cutting edge l. The following equations are presented to calculate the upper boundary of these two values, assume the maximum scallop tolerance to be t_m.

$$a_{p(max)} = l - t_m$$
$$a_{e(max)} = 2\sqrt{R^2 - (R - t_m)^2} \tag{2.16}$$

To our anticipation, a small value of the two parameters will definitely increase the energy consumption ratio for its lower machining efficiency. However, it is not as expected that large cutting depths do not directly lead to a better energy performance, even though the cutting energy (see Fig. 6b) shows a descending trend upon
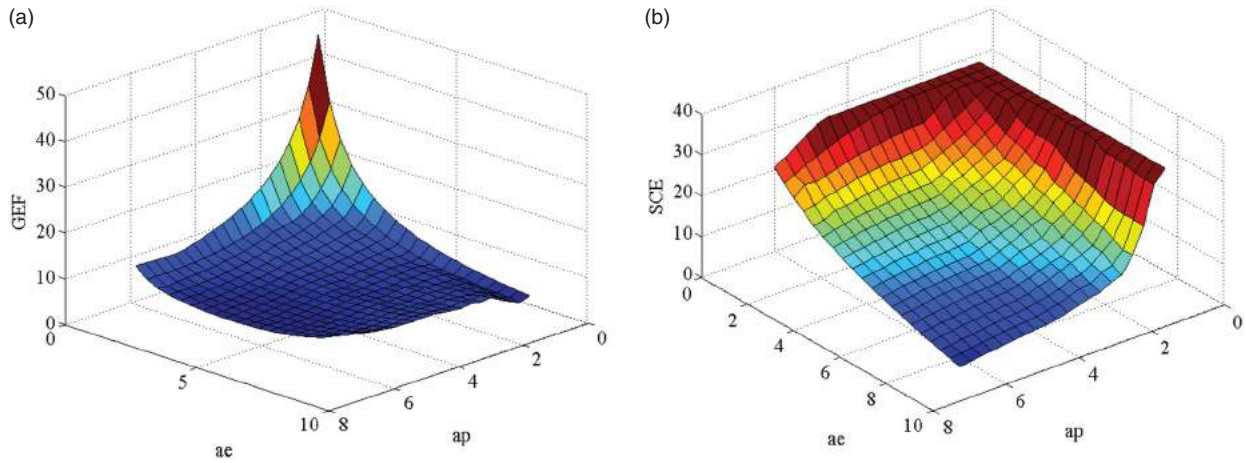
(a)

(b)

Figure 6. The behavior of (a) GEF; (b) SCE, upon different radial and axial depth of cut.

larger values of cutting depths, the decreased feed rate (to keep cutting force under a critical value) in such condition slows down the machining rate, causing more energy consumption on idle running. Therefore, the optimization of the cutting parameters is essentially a trade-off issue, the local optimum in this bounded region is easily obtained by classic algorithms like steepest descend method and Newton iteration method, etc.

Consequently, the optimal set of a_p&a_e is located somewhere in the middle, with which an energy-saving tool path is attainable. And we will explain the tool path strategy in the next section.

3. Tool path planning strategies

In most cases, especially for those blades and dies with a relatively flat surface, a 3-axis machine is capable enough to be tasked with a surface roughing. Unlike the finishing process with only one or two layers of material to be cut on the workpiece, the roughing process usually starts with a raw block with a large volume of material to be removed, which is pretended to be of a fixed value V_r back in Eqn. (2.12). Next, based on the optimal cutting parameters derived in last section, we will provide two different strategies to generate tool path in this section, and give a comparison in the next section.

3.1. Improved constant Z-level strategy

Normally in roughing stage, a simple tool path strategy developed from pocket machining is acceptable, that the model is sliced into several layers with a uniform interval, and the 2D pocket tool path is generated for each layer.

The advantage of the pocket tool path is that an optimal set of radial and axial depth of cut can be always maintained along the tool path, so that a minimum

energy consumption is ensured. However, the surface quality is closely related to the interval between two adjacent layers, i.e. the axial depth of cut a_p, usually the optimal value of it may not be small enough to produce a good surface finish, thus the stair-step shape left on the model (shown in Fig. 7 below) may cause huge vibration in the subsequent finishing process.
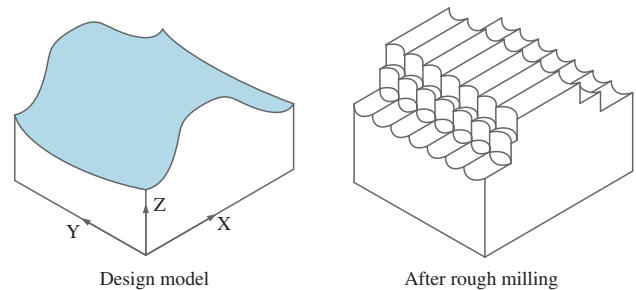

Design model   After rough milling

Figure 7. The stair shape left on the model after rough milling.

Because of this drawback of traditional constant Z-level method, we propose an enhanced strategy that one more special layer of tool path is added at the end, so that these annoying stairs can be swept out. The following procedures explain the whole algorithm of this strategy:

Input: Design model (surface S), Optimal a_p&a_e, Machining tolerance t_m (constant margin value m + cusp height value h).

Output: A group of tool paths for roughing based on the improved constant Z-level strategy.

Step1: Calculate the height h_s of the raw block along Z direction, starting from the top plane of the block, generate a series of planes (excluding the top plane) with a constant interval a_p, the number of planes equals to: $ceil((h_s + t_m)/a_p) - 1$. For each plane, do the intersection operation with S_m, and store the intersection curves i.e. the contours in database $Contour_Z$.
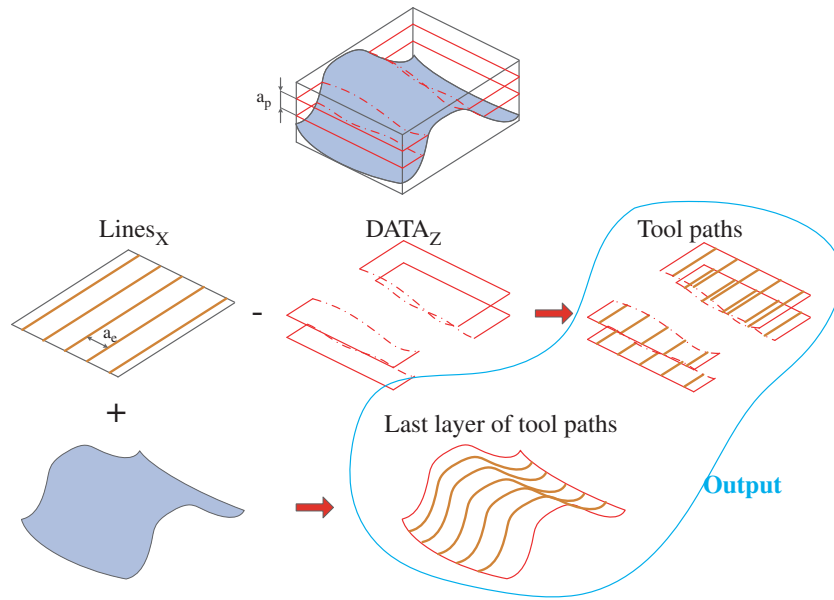
Figure 8. Procedures for the subtraction operation.

Step2: Generate a group of parallel line segments $Lines_X$ along X direction within X-Y plane, eliminate the part outside the surface region, the interval between each two segment is a_e.

Step3: For each contour in $Contour_Z$, do a subtraction boolean operation with $Lines_X$, remove the part of $Lines_X$ that locates inside of the contour curve, lift $Lines_X$ to the corresponding Z-level, and the remaining part of $Lines_X$ is actually the tool paths (CL curves) for that layer, shown in Fig. 8.

Step4: For each point of $Lines_X$, find the corresponding Z value on S_m, the combination of these two data sets generates the last layer of tool path.

Unlike the previous tool paths, the tool path of the last layer is essentially a compromise which aims to eliminate the stair-steps and improve the surface quality. A simulation example will be presented in the next section to judge whether this compromise has a significant influence on the total energy consumption.

We have generated the entire tool paths by this strategy, the data structure is described by the following equation, note that the row index represents the layer, and each tool path Tp_{ij} is a set of discrete points $\{x_k, y_k, z_k\}$.

$$Toolpathdata = \begin{Bmatrix} Tp_{11} & \cdots & Tp_{1m} \\ \vdots & \ddots & \vdots \\ Tp_{n1} & \cdots & Tp_{nm} \end{Bmatrix} \quad (3.1)$$

3.2. Optimized morphing strategy

Even though the improved constant Z-level strategy could maintain an optimal energy consumption during most of the time (except for the last cutting layer), it is only workable for those surfaces with small fluctuation. For an arbitrary free-form surface like a sinusoidal surface, it is predictable that the cutter will suffer from a frequent vertical movement even in a single tool path, this "lifting" action will cause a slot cutting which is not only unpredictable by the presented energy model, but also detrimental to the cutter itself. Based on the above concerns, another strategy named "optimized morphing strategy" is proposed here.

Morphing technique is widely used in motion pictures and movies, changing one shape into another through seamless transition. We borrow this concept into the tool path planning so that a raw block can be machined into the design model during a smooth transition. Moreover, for a specific surface, an optimal direction always exists which has the minimum fluctuation of Z, an optimal value of a_p can be thus largely maintained along this direction. For the example shown below (Fig. 9), direction A is certainly superior to B.

Before describing the detailed steps of the tool path strategy, we should first create a mathematical model to represent the fluctuation. For a given direction α in X-Y plane, we can generate a curve right on the surface whose projection in X-Y plane is along α. For a particular curve $\{x_i, y_i, z_i\}$, the fluctuation can be expressed as:

$$fluc = \frac{\sum_{i=2}^{n} abs(z_i - z_{i-1})}{\sum_{i=2}^{n} norm(x_i - x_{i-1}, y_i - y_{i-1}, z_i - z_{i-1})} \quad (3.2)$$

Where the denominator is actually the approximate curve length, and the numerator is the accumulated
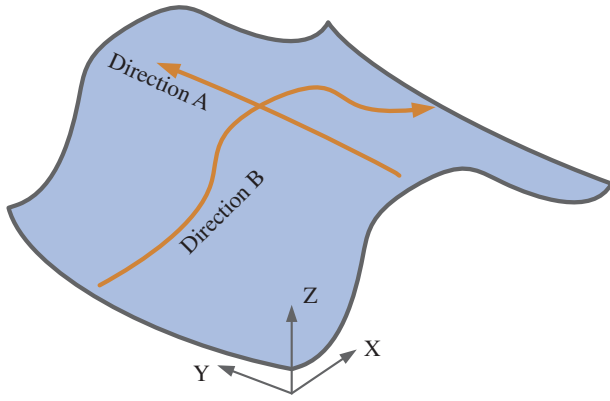
Figure 9. Difference of cutting direction in terms of fluctuation in Z direction.

Figure 10. One list of morphing tool path from the bottom-up.

fluctuation value along this curve. The optimal direction α with least fluctuation can be thus determined by brutal force, and the full steps for tool path generation are shown below:

Step1: Parallel to the direction α and Z axis, generate a set of parallel planes with a constant interval a_e, their intersection with S_m will produce a set of curves. We name these curves leading curves.

Step2: Find an optimal direction α_{opt}, such that the summation of fluctuation for each leading curve, i.e. $\sum fluc$ is minimized. Save these optimal leading curves as $\{LC_{1,1}, LC_{1,2} \dots LC_{1,m}\}$.

Step3: For each leading curve $LC_{1,k}\{x_i, y_i, z_i\}$, go back to step1 to find the plane P_k that contains LC_k, generate a group of morphing curves right on P_k, the total number of curves (including the leading one) is calculated by:

$$n_k = \text{round} \left(\frac{\max(z_{top} - z_i) + \min(z_{top} - z_i)}{2a_p} \right) \quad (3.3)$$

Step4: Use linear interpolation to define morphing levels. In a mathematical description, starting from the leading curve $LC_{1,k}\{x_i, y_i, z_i\}$, the upper curve $LC_{1+j,k}$ can be represented by:

$$LC_{1+j,k} = \left\{ x_i, y_i, z_i + \frac{(z_{top} - z_i)j}{n_k} \right\} \quad (3.4)$$

So far, all the curves generated can be regard as CL curves, Fig. 10 demonstrates the tool path generation starting from the leading curve.

As a conclusion, two different strategies for tool path planning are proposed, the first strategy performs a best energy consumption during most of the time, however only suitable for machining surfaces with less fluctuation; the second strategy can be utilized into arbitrary free-form surfaces, but may consume a higher energy.
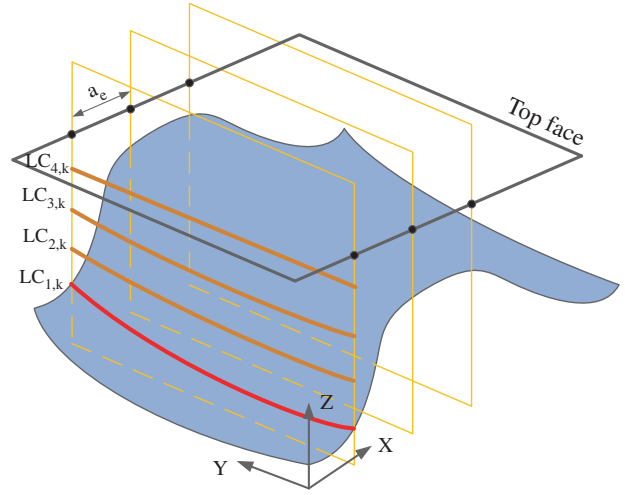
In next section, a virtual surface will be machined by both strategies, an exhaustive comparison will be made accordingly.

4. Simulation results

The whole methodology has been implemented and verified in MATLAB, where a group of simulated experiments is conducted. The design surface is a Bezier Surface generated by a 5*5 control point set, with both concave and convex features, shown in Fig. 11. A Z-dimensional vector (ZDV) method is utilized to virtually represent the in-progress workpiece, an initial bunch of vectors along Z direction with equal height is planted covering the entire surface. These vectors are progressively mowed and updated with a shorter height when the tool moves along the tool path. By calculating the geometric intersection between each ZDV and a ball-end tool (which is purely represented as the combination of a half sphere and a cylinder), the cutting depths as well as the cutter-workpiece engagement are easily obtained. The real-time workpiece profile is numerically simulated by the remainder of the ZDVs.

Machine tool parameters are manually selected based on an average configuration of state of art vertical machine centers with ball-end mills, shown in Tab. 1. Al7039-T64 is chosen as the workpiece material, of which the cutting force coefficients are determined by curve fitting technique according to the calibrated data in [23]. Regarding the cutting force, we set the critical force value as 700N, such that feed rate is constrained by both mechanics and kinematics limitations. Machine tolerance is chosen to be $1 \sim 2$ mm, as there is no need to strictly constrain the cusp value, overcut however, is not allowed in rough milling. Tab. 2 lists the assumptions we

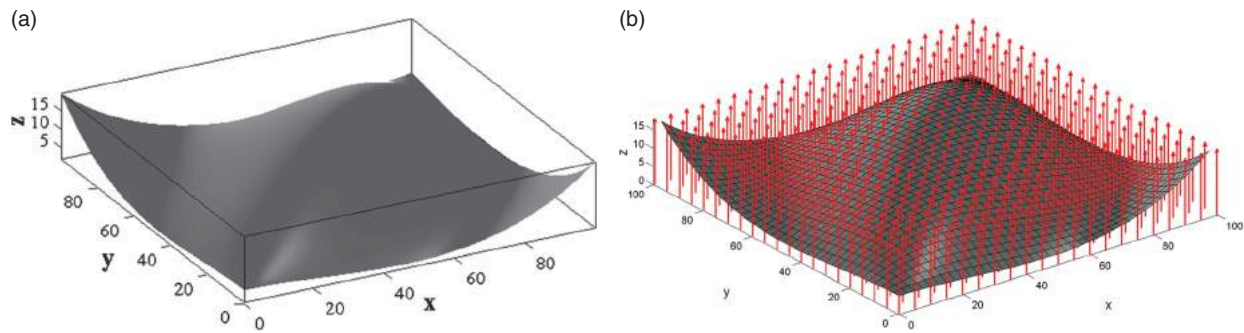(a)

(b)

Figure 11. (a): Design surface generated by 5*5 control points; (b): workpiece represented by ZDVs.

Table 1. Machine and Tool configuration.

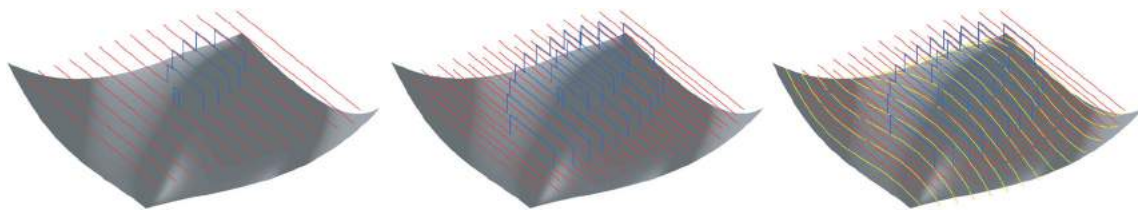| Machine configuration			Tool parameters			
Spindle speed	Maximum allowable feed rate	Idle power	Radius (R)	Helix angle (i_0)	Cutting edge number	Maximum cutting depth
3000RPM	2000mm/min	1.5KW	6mm	30°	4	10mm

Figure 12. Generated tool paths based on improved constant Z-level strategy.

have made through the whole modeling and simulation, serving as the priority for this research. Real conditions are subjected to change with unpredictable factors, such as the idle power slightly varies with different feed rate in practice, these changes are considered to be minor and less influential to the credibility of the simulation results.

After all these parameters are set, the GEF can be obtained by Eqn. (2.12), Fig. 6 has already shown the corresponding GEF previously. The optimal values of a_p&a_e according to this figure, locates inside the range of 4.5 mm and 7 mm, when the value of GEF can be minimized.

The proposed two strategies for tool path planning are implemented in this example, Figs. 12 and 13 show the corresponding tool paths respectively. As for the first strategy, totally three layers of tool paths are generated, the last layer (plotted in yellow) is the special layer to eliminate the stair-steps created by the first two layer of tool path, the blue lines are the tool path for rapid movement where the tool has no physical contact with the workpiece. On the other side, tool paths generated by optimized morphing strategy are displayed in Fig. 13, where the tool paths are forced along an optimal direction, it is obvious that along this direction the surface has smaller fluctuation vertically. The leading curves are shown in yellow, a set of subsequent red tool paths are generated afterward. Different from the first strategy, the number of curves for each set varies, producing a morphing change from a raw block to a semi-finished surface.
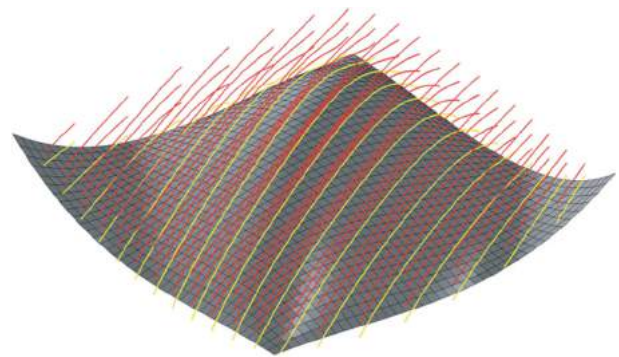

Figure 13. Generated tool paths based on optimized morphing strategy.

The total energy consumptions by these two strategies are estimated according to the proposed model. For the first strategy, we assume that the tool moves with a maximum speed, i.e. the maximum allowable feed rate, during rapid movement along those blue curves, only idle power will be considered. For those red and yellow curves, where real cutting event happens, we calculate the average GEF value for each two adjacent CL points and the swept volume when the tool moves from one point to another, so that the estimated total energy consumption
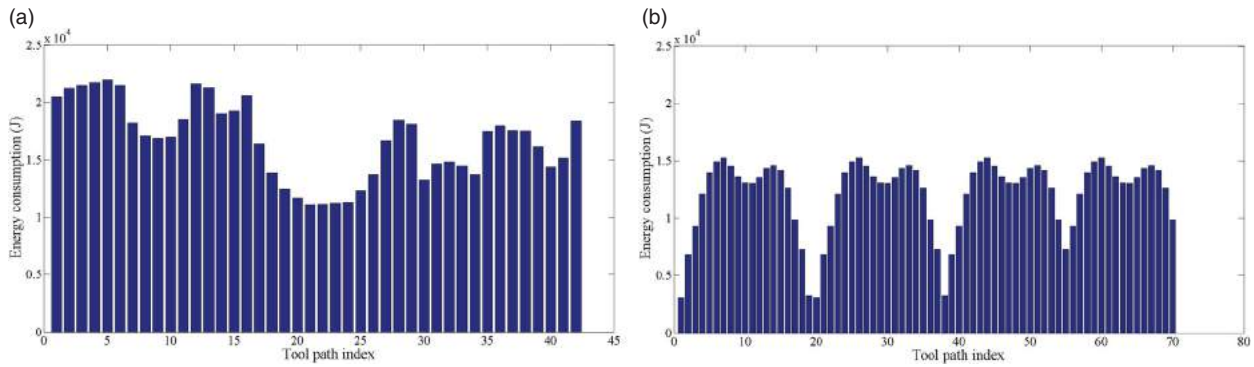
(a)

(b)

Figure 14. Histograms of energy consumption for optimal a_p&a_e: (a) Strategy 1, (b) Strategy 2.

Table 2. Preliminary assumptions.

Idle Power	Kept as constant
Initial workpiece	Block
Surface quality constraint	Maximum scallop height should be less than the machine tolerance
Uncut moving speed	Maximum allowable feed rate

can be expressed as:

$$E_{total} = \sum \frac{GEF_i + GEF_{i+1}}{2}$$
$$\cdot \frac{(a_{p(i+1)}a_{e(i+1)} + a_{p(i)}, a_{e(i)})\boldsymbol{p_{i+1}} - \boldsymbol{p_i}}{2} \quad (4.1)$$

Where: $\boldsymbol{p_i}$ represents the coordinate of CL point. Based which, the following results for each strategy can be calculated and compared accordingly.

Figure 14 shows the energy consumption values for every single tool path, the total energy consumption can be calculated as a summation. To be expected, as the first strategy maintains an optimal GEF value most of the time, it is undoubtedly more energy efficient. The second strategy consumes 20% more energy than the first one. Unexpectedly, even though the total curve length of the second strategy is 46% longer than the first one, the total machining time is only slightly larger than the first one. A reasonable explanation is that feed rate becomes larger during some of the machining periods. As we can observe

from Fig. 13, around the middle area of the surface, the cutting depth a_p, i.e. the vertical interval between two curves decreases, producing a small chip load, feed rate is thus increased to maintain a fairly stable cutting force.

Traditionally in rough milling, usually a maximum value of a_p&a_e is recommended for large productivity. The energy consumed by idle power will be definitely lowered upon large productivity, however the total energy consumption pattern is still unknown under this circumstance. Therefore another comparison is made between the optimal and traditional cutting parameters. To keep it fair we will use the proposed tool path strategies for both conditions. The maximum allowable axial and radial depth of cut are determined by Eqn. (2.16), values regarding machine tolerance are 8 mm and 7 mm, respectively. Figs. 15 and 16 display the tool paths with the maximum a_p&a_e value, this time, due to the increased value of a_p, only two layers of tool paths are generated. Fig. 16 and Tab. 3 give results for both strategies. Compared with Tab. 4, the total curve length has a remarkable decrease, whereas the productivity as well as energy efficiency shows no more advantages, both have a significant increase, especially for strategy 1.

As a conclusion, we virtually established a vertical machine center, a ball-end tool, and a free-form surface to be machined. Under the mechanics and kinematics constraints, two key cutting parameters: axial
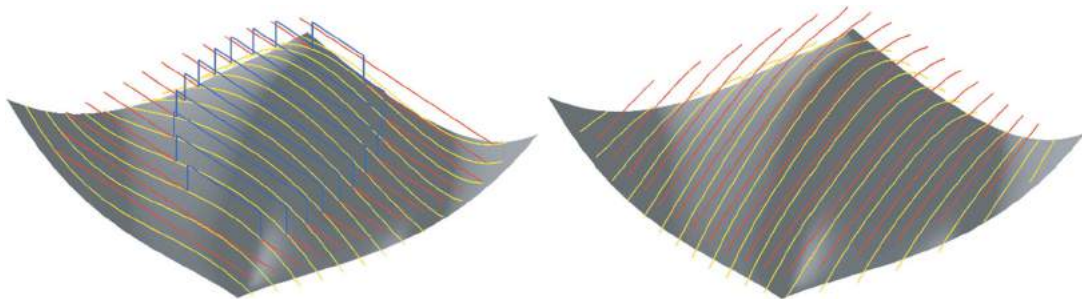

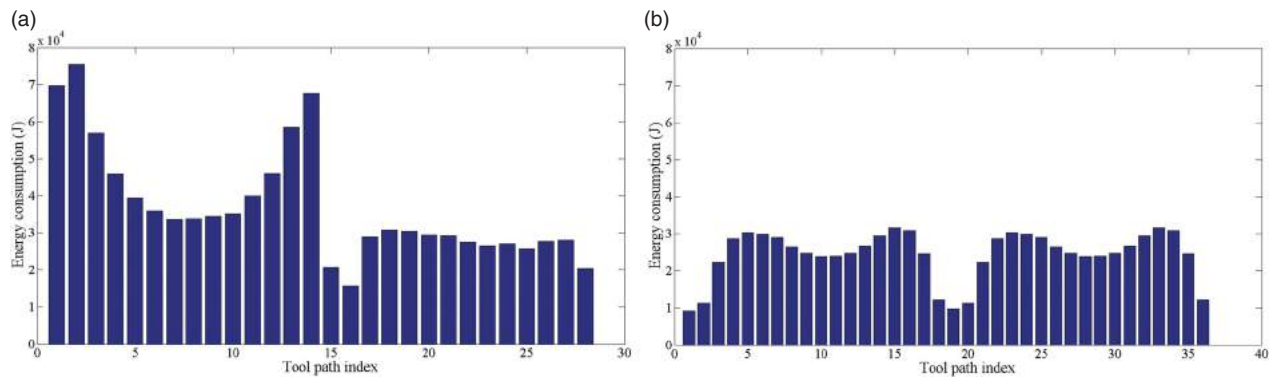**Figure 15.** Tool paths generated by two strategies with a maximum value of a_p&a_e.

Figure 16. Histograms of energy consumption for maximum a_p&a_e: (a) Strategy 1, (b) Strategy 2.

Table 3. Simulation results between two strategies for maximum a_p&a_e.

Maximum a_p&a_e	Total energy consumption	Total curve length	Total machining time
Strategy 1	1040KJ	2871.8mm	625.6s
Strategy 2	881KJ	3214.0mm	402.5s

Table 4. Simulation results between two strategies for optimal a_p&a_e.

Optimal a_p&a_e	Total energy consumption	Total curve length	Total machining time
Strategy 1	702KJ	4328.9mm	324.3s
Strategy 2	852KJ	6352.6mm	387.8s

and radial depth of cut, are optimized by the GEF function. Comprehensive comparisons of tool paths, energy efficiency and productivity are made between two proposed tool path planning strategies upon optimal and maximal cutting parameters. The first strategy shows a best energy and productivity performance when equipped with the optimal cutting parameters, but produces a worst performance with the maximum a_p&a_e. The second strategy gives moderate performance for both optimal and maximum cutting parameters.

In real machining of surface roughing, for surfaces with abrupt concave and convex features like car body molds, strategy 1 is always preferred as it maintains a fixed set of cutting parameters most of the time, which is assumed to be the most energy efficient combination; however for flat surfaces with small twisting features like blade surface, both strategies exhibit no big difference on the energy performance, and the morphing strategy is more preferred if one wants to increase the productivity without sacrificing much energy consumption, as the tool path is naturally smoothed without any "tool lifting" movements, the machining time is therefore remarkably saved compared with strategy 1.

5. Conclusion and future work

Two energy-saving strategies for 3-axis tool path planning are proposed in this paper. Tool path for surface roughing, compared with surface finishing, is relatively simple-fashioned with less variables: radial depth of cut a_e and axial depth of cut a_p. Therefore, the optimization of these two variables has been studied in the first place. An energy consumption model including cutting power demand and idle power demand is established first. By considering cutting torque and cutting volume during one spindle turn, a mathematical model is derived to describe the specific cutting energy. After that, together with idle power, a global energy consumption formula (GEF) is created as a function of the two cutting parameters, while the upper bound of feed rate is constrained by the critical cutting force value. By this formula, the specific energy consumption for a given machine tool configuration can be easily estimated and optimized. A group of preliminary simulations shows that the optimal parameters together with the proposed tool path generation methods can save up to 30% of the total energy usage compared with traditional cutting parameters.

Nevertheless, the presented approach only gives a rough, more works such as cutting force calibration and real machining tests should be done to make it valid. In the future more cutting experiments will be conducted in real CNC platform, and we will further go deeply into the energy optimization for complex surface finishing.

ORCID

Ke Xu ⓘ http://orcid.org/0000-0003-4934-1837
Kai Tang ⓘ http://orcid.org/0000-0002-5184-2086

References

[1] Bao, W.; Tansel, I.: Modeling micro-end-milling operations. Part I: analytical cutting force model, International Journal of Machine Tools and Manufacture, 40, 2000, 2155–2173. http://dx.doi.org/10.1016/S0890-6955(00)00054-7

[2] Beudaert, X.; Lavernhe, S.; Tournier, C.: Feedrate interpolation with axis jerk constraints on 5-axis NURBS and G1 tool path, International Journal of Machine Tools and Manufacture, 57, 2012, 73–82. http://dx.doi.org/10.1016/j.ijmachtools.2012.02.005

[3] Diaz, N.; Redelsheimer, E.; Dornfeld, D.: Energy consumption characterization and reduction strategies for milling machine tool use, Glocalized Solutions for Sustainability in Manufacturing, 2011, 263–267

[4] Dietmair, A.; Verl, A.: Energy consumption forecasting and optimisation for tool machines, Energy, 62, 2009, 63

[5] Ding, S.; Mannan, M.; Poo, A. N.; Yang, D.; Han, Z.: Adaptive iso-planar tool path generation for machining of free-form surfaces, Computer-Aided Design, 35, 2003, 141–153. http://dx.doi.org/10.1016/S0010-4485(02)00048-9

[6] Draganescu, F.; Gheorghe, M.; Doicin, C.: Models of machine tool efficiency and specific consumed energy, Journal of Materials Processing Technology, 141, 2003, 9–15. http://dx.doi.org/10.1016/S0924-0136(02)00930-5

[7] Engin, S.; Altintas, Y.: Mechanics and dynamics of general milling cutters.: Part I: helical end mills, International Journal of Machine Tools and Manufacture, 41, 2001, 2195–2212. http://dx.doi.org/10.1016/S0890-6955(01)00045-1

[8] Erdim, H.; Lazoglu, I.; Ozturk, B.: Feedrate scheduling strategies for free-form surfaces, International Journal of Machine Tools and Manufacture, 46, 2006, 747–757. http://dx.doi.org/10.1016/j.ijmachtools.2005.07.036

[9] Feng, H.-Y.; Su, N.: Integrated tool path and feed rate optimization for the finishing machining of 3D plane surfaces, International Journal of Machine Tools and Manufacture, 40, 2000, 1557–1572. http://dx.doi.org/10.1016/S0890-6955(00)00025-0

[10] Han, Z.; Yang, D. C.: Iso-phote based tool-path generation for machining free-form surfaces, Journal of manufacturing science and engineering, 121, 1999, 656–664. http://dx.doi.org/10.1115/1.2833094

[11] Kara, S.; Li, W.: Unit process energy consumption models for material removal processes, CIRP Annals-Manufacturing Technology, 60, 2011, 37–40. http://dx.doi.org/10.1016/j.cirp.2011.03.018

[12] Kim, G.; Cho, P.; Chu, C.: Cutting force prediction of sculptured surface ball-end milling using Z-map, International Journal of Machine Tools and Manufacture, 40, 2000, 277–291. http://dx.doi.org/10.1016/S0890-6955(99)00040-1

[13] Kim, T.; Sarma, S. E.: Toolpath generation along directions of maximum kinematic performance; a first cut at machine-optimal paths, Computer-Aided Design, 34, 2002, 453–468. http://dx.doi.org/10.1016/S0010-4485(01)00116-6

[14] Kurt, M.; Bagci, E.: Feedrate optimisation/scheduling on sculptured surface machining: a comprehensive review, applications and future directions, The International Journal of Advanced Manufacturing Technology, 55, 2011, 1037–1067. http://dx.doi.org/10.1007/s00170-010-3131-3

[15] Larue, A.; Altintas, Y.: Simulation of flank milling processes, International Journal of Machine Tools and Manufacture, 45, 2005, 549–559. http://dx.doi.org/10.1016/j.ijmachtools.2004.08.020

[16] Lauwers, B.; Lefebvre, P.: Five-axis rough milling strategies for complex shaped cavities based on morphing technology, CIRP Annals-Manufacturing Technology, 55, 2006, 59–62. http://dx.doi.org/10.1016/S0007-8506(07)60366-7

[17] Lee, P.; Altintaş, Y.: Prediction of ball-end milling forces from orthogonal cutting data, International Journal of Machine Tools and Manufacture, 36, 1996, 1059–1072. http://dx.doi.org/10.1016/0890-6955(95)00081-X

[18] Lefebvre, P. P.; Lauwers, B.: 3D morphing for generating intermediate roughing levels in multi-axis machining, Computer-Aided Design and Applications, 2, 2005, 115–123. http://dx.doi.org/10.1080/16864360.2005.10738359

[19] Lo, C.-C.: Efficient cutter-path planning for five-axis surface machining with a flat-end cutter, Computer-Aided Design, 31, 1999, 557–566. http://dx.doi.org/10.1016/S0010-4485(99)00052-4

[20] Mouzon, G.; Yildirim, M. B.; Twomey, J.: Operational methods for minimization of energy consumption of manufacturing equipment, International Journal of Production Research, 45, 2007, 4247–4271. http://dx.doi.org/10.1080/00207540701450013

[21] Newman, S. T.; Nassehi, A.; Imani-Asrai, R.; Dhokia, V.: Energy efficient process planning for CNC machining, CIRP Journal of Manufacturing Science and Technology, 5, 2012, 127–136. http://dx.doi.org/10.1016/j.cirpj.2012.03.007

[22] Ozturk, B.; Lazoglu, I.: Machining of free-form surfaces. Part I: Analytical chip load, International Journal of Machine Tools and Manufacture, 46, 2006, 728–735. http://dx.doi.org/10.1016/j.ijmachtools.2005.07.038

[23] Ozturk, B.; Lazoglu, I.; Erdim, H.: Machining of free-form surfaces. Part II: Calibration and forces, International Journal of Machine Tools and Manufacture, 46, 2006, 736–746. http://dx.doi.org/10.1016/j.ijmachtools.2005.07.037

[24] Quintana, G.; Ciurana, J.; Ribatallada, J.: Modelling power consumption in ball-end milling operations, Materials and Manufacturing Processes, 26, 2011, 746–756. http://dx.doi.org/10.1080/10426910903536824

[25] Sencer, B.; Altintas, Y.; Croft, E.: Feed optimization for five-axis CNC machine tools with drive constraints, International Journal of Machine Tools and Manufacture, 48, 2008, 733–745. http://dx.doi.org/10.1016/j.ijmachtools.2008.01.002

[26] Suresh, K.; Yang, D.: Constant scallop-height machining of free-form surfaces, Journal of Engineering for Industry, 116, 1994, 253–259. http://dx.doi.org/10.1115/1.2901938

[27] Toh, C.: Cutter path strategies in high speed rough milling of hardened steel, Materials & design, 27, 2006, 107–114. http://dx.doi.org/10.1016/j.matdes.2004.09.021

[28] Zhang, L.; Feng, J.; Wang, Y.; Chen, M.: Feedrate scheduling strategy for free-form surface machining through an integrated geometric and mechanistic model, The International Journal of Advanced Manufacturing Technology, 40, 2009, 1191–1201. http://dx.doi.org/10.1007/s00170-008-1424-6